ENERGY DETECTION TROPOSCATTER SYSTEM WITH INBAND DIVERSITY

By
Capt. M. JAYAKRISHNAN

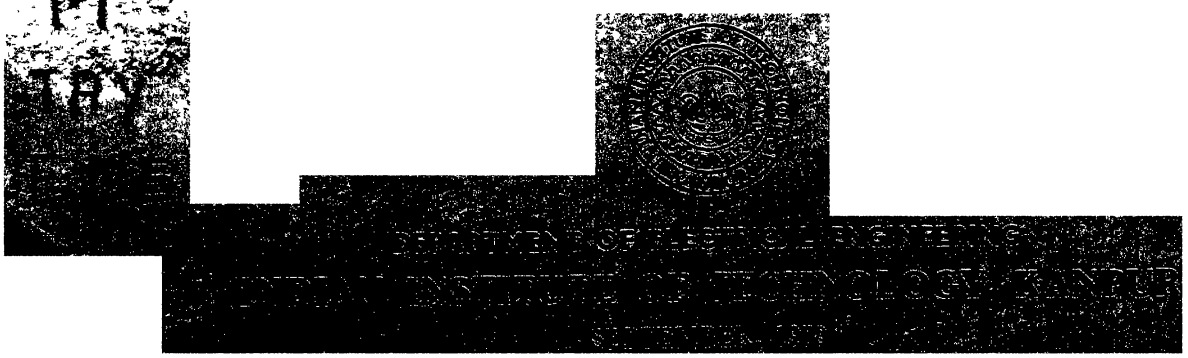

ENERGY DETECTION TROPOSCATTER SYSTEM WITH INBAND DIVERSITY

A Thesis Submitted
in Partial Fulfilment of the Requirements
for the Degree of
MASTER OF TECHNOLOGY

By
Capt. M. JAYAKRISHNAN

to the
DEPARTMENT OF ELECTRICAL ENGINEERING
INDIAN INSTITUTE OF TECHNOLOGY, KANPUR
SEPTEMBER, 1978

EE-1978-M-JAY-ENE

CERTIFICATE

This is to certify that the thesis entitled 'Energy Detection Troposcatter System with Inband Diversity' is a record of the work carried out by Capt. M. Jayakrishnan under my supervision and that it has not been submitted elsewhere for a degree.

Dr. P.K. Chatterji
Assistant Professor
Department of Electrical Engineering
Indian Institute of Technology
Kanpur.

23 September, 1978

ACKNOWLEDGEMENTS

I am greatly indebted to Dr. P.K. Chatterji for his constant and valuable guidance in the preparation of this thesis. He has evinced keen interest at every stage and helped me to complete this thesis.

I would like to gratefully acknowledge all the help given by Dr. V.P. Sinha and Dr. M.S. Krishnamurthy at various stages during the preparation of this thesis.

I am also deeply obligated to Dr. V. Rajaraman, Dr. R. Sankar and Dr. P.R.K. Rao who taught me during my stay here.

I am singularly indebted to Lt.Col. Gurudev Singh for his valuable assistance while preparing and running the many computer programmes involved in this thesis. I have also drawn freely upon the skills of my colleagues and friends in preparing this thesis. Since the list of these becomes too extensive to permit individual acknowledgements, let each of them accept my sincere thanks for helping me in this effort.

Finally, I also acknowledge with pleasure the excellent typing by Mr. C.M. Abraham.

LIST OF CONTENTS

ABSTRACT

Reliable communications over fading dispersive channels requires the utilization of some form of diversity. Possible diversity techniques suitable for mobile troposcatter systems are examined, with particular emphasis on inband diversity. Some inband frequency diversity techniques are simulated and error probabilities are obtained for various SNRs. These error probabilities are usually less than those obtained by Bello [3].

CHAPTER 1

INTRODUCTION

In recent years, a tactical troposcatter system on wheels, is a very attractive proposition for reliable communications. This is especially true, when satellite communication for military usage on a large scale becomes prohibitive in cost. A mobile troposcatter system is characterized by the constraints that it imposes on the size of the system. A troposcatter channel is characterized by the presence of fading and multipath besides the usual additive noise. Hence reliable communication over such fading dispersive channels requires the utilization of some form of diversity.

1.1 Peculiarities of a Mobile Troposcatter System

A mobile troposcatter system imposes certain constraints due to the mobile role it has to play. Mobility in this case implies ease of transportability. A mobile troposcatter system should be capable of being transported conveniently and the establishment of a communication link should be possible within a short time. These two basic requirements of a mobile troposcatter system effects many aspects in the design of the system. The first, involves a reduction in the size and bulk of the equipment. Therefore, the design should bepreferably be based on a single transmitter and receiver using only one antenna. Since the power plant has

also got to be mobile, there is a limitation on the amount of power available. The utilization of conventional forms of diversity like space and frequency involves increasing the size of the system to accommodate the dual antennas as in space diversity or the dual transmitters as in frequency diversity. These are, therefore, not advantageous in a mobile troposcatter system. The second requirement of establishment of the link in minimum possible time results in limited alignment time. This is particularly so in conventional space and frequency diversity techniques where there are more than one antenna to be aligned.

A consistently higher degree of message recovery always involves some form of diversity technique . Hence, in the case of a mobile troposcatter system we therefore need some technique of diversity that does not have any of the constraints mentioned earlier. Some of the possibilities are :

a) Angle diversity
b) Polarization diversity
c) Time diversity
d) Multipath diversity
e) In band diversity including modified forms of frequency diversity.

These are dealt with in greater detail in the next section.

1.2 Diversity Techniques Suitable for Mobile Tropo

1.2.1 Angle Diversity

Angle diversity can be considered as a form of space diversity. While space diversity is obtained by the relative phasing among rays from one portion of the scatter volume, in angle diversity a number of transmitting beams are used each oriented towards a non overlapping portion of the scatter volume and a similar number of receiving beams associated with each transmitting beam. This does not require any additional antennas, though a number of feed cones are required at each antenna. Additional transmitter power is necessary. Angle diversity is considered as one of the best ways of achieving diversity nowadays in the context of mobile tropo systems [9].

1.2.2 Polarization Diversity

In this case we transmit signals polarized in one plane. In the channel depolarization occurs. The signal is received independently on two orthogonal polarizations. The two received signals do not fade in a correlated manner. Since there are only two orthogonal polarization modes, this is essentially a dual diversity technique. However, this technique is not useful in troposcatter since there is hardly any change in the polarization while the wave propagates. However, since the polarization does not change while propagating it is possible to consider transmitting orthogonal polarizations and receiving them separately [4].

1.2.3 Time Diversity

In time diversity, the same information is repetitively transmitted at time intervals well separated as compared to the reciprocal of the average fading rate. Since the channel is time selective, the fade levels associated with the various repetitions will essentially be independent. Hence, appropriate combinations of the repetition will give a diversity performance. Unlike techniques like space diversity, time diversity is achieved without any increase to the total average received power per bit.

1.2.4 Multipath Diversity

This is another form of time diversity that can be achieved in situations where sufficiently wideband signals are transmitted and the multipath may be viewed as creating a series of echoes. The contributions ariving via the different parts of the multipath structure can be seperated in the course of reception and combined in diversity. The Rake system uses such a technique. Here the received signal plus noise is cross correlated against a replica of each possible transmitted waveform, at every possible delay and the results summed with a maximal ratio combiner weighting using the estimate of the channel at that relative delay [4].

1.2.5 Inband Diversity

This is the diversity implicit in the channel due to the

time and frequency selective fading that the signal undergoes in the channel. This is possible due to the fact that pulses at different frequencies fluctuate in an uncorrelated manner. Thus if we transmit the same information at different frequencies, we have an inband frequency diversity. Unlike the conventional frequency diversity technique where the seperation in frequency is larger, here we use a small seperation in frequency to achieve the effect of diversity.

1.3 Energy Detection

In order to obtain high data rates and reliable transmission on fading dispersive channels like troposcatter links, clever use must be made of the diversity inherent in the available transmission bandwidth. The basic approach is to transmit pulses whose time duration and/or bandwidth cover many selective fades in time and/or frequency and to use energy detection for pulse discrimination [3].

It is possible to have both time and inband frequency diversity using energy detection. However, since the pulse width is very small compared to the fading time constant, time diversity is unsuitable as a large duration has to elapse to get two uncorrelated pulses. This means that the time between two uncorrelated pulses is very large and this results in very low data rates.

However, if we use different frequencies in small time slots it is possible to achieve frequency diversity without much loss in data rate. Here the bandwidth of the pulses is larger than the coherent bandwidth of the channel. The use of time-frequency pattern is one such technique. Here the spectral energy in the vicinity of the mark frequency is identified as mark and the energy around the space frequency as space.

Consider a non coherent FSK case with multiplicative fading occuring at a rate faster or comparable to the pulse rate. If T is the symbol duration and T_a the nominal width of the normalized autocovariance of the complex Gaussian fading process, then over each symbol duration we have

$$M = \frac{T}{T_a} \qquad (1.1)$$

independently fading states occuring. Each of these M successive outputs spaced at intervals of T_a are independent complex zero mean Gaussian variates, each having a signal and a noise component. Now if we have filters centered around mark and space frequencies and the samples of each filter square law combined over the symbol duration T, we can arrive at a decision based on the larger of the combined outputs. This in brief is the principle of energy detection.

While it is possible to use other forms of diversity like angle diversity and polarization diversity in a mobile

troposcatter system, one of the attractive methods is utilizing inband diversity using energy detection. This does entail a loss in data rate due to repeating the same information within a fixed bandwidth allocation. However, it should be possible to achieve high data rates using good coding and decoding techniques.

1.4 Scope of the Work

The simulations reported here pertain to the study of inband frequency diversity using energy detection. We use a channel model as described in [2] for this simulation. The parameters of the link are as would be found in the case of a mobile troposcatter link and is described later. The channel characterization is discussed in Chapter 2. In Chapter 3, we discuss the complex digital filtering techniques used here and the generation of complex Gaussian samples. In Chapter 4, the energy detection system and the different signalling formats for inband diversity are discussed. We have simulated three different time-frequency formats and the relative advantages of each are dealt with here. Chapter 5 deals with the simulation. The flow-chart is discussed here in detail, and results are discussed. In Chapter 6, we conclude this thesis.

CHAPTER 2

CHANNEL CHARACTERIZATION

2.1 Introduction

All radio transmission media may be considered as a randomly time variant linear channel. In a radio channel, like in any linear system, the transfer function or the impulse response provides necessary information for characterizing its input-output behaviour. Since the system functions are random processes that are at most quasi-stationary, such a characterization is complex. One such idealized statistical model for representing fading dispersive radio channel is the Gaussian wide sense stationary uncorrelated scattering (WSSUS) model [1].

Certain simplifications can be made to the general characterization of the randomly time variant channel, while transmitting digital signals. The simplifications become possible when the time and frequency selective behaviour of the channel may be regarded as wide sense stationary for time intervals much larger than the durations of the signalling waveforms that are being used. Such a situation arises when the channel contains very slow fluctuations superimposed upon more rapid fluctuations, which exhibit stationarity properties.

2.2 Gaussian WSSUS Model

The defining characteristics of a Gaussian wide sense stationary uncorrelated scattering model may be expressed as below :

The time variant transfer function is a wide sense stationary complex Gaussian process in both time and frequency variables of the transfer function. That is, if we denote the time variant transfer function by T(f,t), the WSSUS property of the definition becomes

$$E[T^{*}(f,t)\ T(f+\Omega,\ t+\tau)] = R(\Omega,\tau) \qquad (2.1)$$

where $R(\Omega,\tau)$ is the time frequency correlation function.

The time variant transfer function T(f,t) is the Fourier transform of the time varying impulse response $g(t,\xi)$.

$$T(f,t) = \int g(t,\xi)\, e^{-j2\pi f\xi}\, d\xi \qquad (2.2)$$

$$g(t,\xi) = \int T(f,t)\ e^{j2\pi f\xi}\, df \qquad (2.3)$$

The magnitude of T(f,t) has a Raleigh distribution function and the phase of T(f,t) is uniformly distributed [2].

From the time frequency correlation function $R(\Omega,\tau)$ we get,

a) the frequency correlation function

$$g(\Omega) = R(\Omega,0) \qquad (2.4)$$

b) the time correlation functions

$$p(\tau) = R(0,\tau) \tag{2.5}$$

Since the channel has uncorrelated scattering from different paths, we have

$$E[g^{*}(t,\xi)\ g(t+\tau,\eta)] = Q(\tau,\xi)\ \delta(\eta-\xi) \tag{2.6}$$

where $\delta(\cdot)$ is the unit impulse response function and $Q(\tau,\xi)$ is proportional to the autocorrelation of the gain functions for paths providing delays in the range $(\xi, \xi + \delta\xi)$ in a tapped delay line model. This function is called the path gain correlation function or tap gain correlation function [2].

$Q(\tau,\xi)$ and $R(\Omega,\tau)$ are Fourier transform pairs.

$$R(\Omega,\tau) = \int Q(\tau,\xi)\ e^{-j2\pi\Omega\xi}\, d\xi \tag{2.7}$$

$$Q(\tau,\xi) = \int R(\Omega,\tau) e^{j2\pi\Omega\xi}\, d\Omega \tag{2.8}$$

2.3 Delay Power Spectrum

The delay power spectrum $Q(\xi)$ as mentioned earlier is the Fourier transform of the frequency correlation function $R(\Omega)$.

$$Q(\xi) = Q(0,\xi) = \int q(\Omega) e^{j2\pi\Omega\xi}\, d\xi\Omega \tag{2.9}$$

Hence, it is equal to the power contained in the channel transfer

function. In other words, the delay power spectrum $Q(\xi)$ is the intensity of scattering for the delay ξ .

Physically it is the cross correlation between two carriers that are seperated by Ω Hz and is a measure of the channel correlation bandwidth. This correlation bandwidth becomes monotonically narrower for a given antenna size as the antenna separation increases, while for a given antenna seperation the correlation bandwidth increases as the size of the antenna increases [4]. From the width of $Q(\xi)$ we can determine the amount of intersymbol interference and the extent of frequency selectivity. This width is the multipath spread of the channel.

2.4 The Tapped Delay Line Channel Model

The WSSUS channel can be modelled as a tapped delay line with taps taken at intervals of $\frac{1}{W_i}$ secs. [1], [4], where W_i is the sampling frequency.

Assuming that the channel responds to frequencies in the interval

$$f_i - W_i/2 < f < f_i + W_i/2,$$

then, we have

$$g(t,\xi) = \sum_{n=-\infty}^{\infty} g(t,n/W_i)\cdot\exp[j2\pi f_c(\xi - n/W_i)]\ x$$
$$\operatorname{sinc}[(\xi - \tfrac{n}{W_i})W_i] \qquad (2.10)$$

given the sample values of $g(t,\xi)$ at time intervals $1/W_i$ apart, where

$$\text{Sinc } y = \frac{\text{Sin } \pi y}{\pi y}$$

If $z(t)$ and $w(t)$ are the complex channel input and output respectively, then we have by convolution,

$$w(t) = \int_{-\infty}^{\infty} z(t-\xi)\, g(t,\xi)\, d\xi \tag{2.11}$$

This results in

$$w(t) = \int_{-\infty}^{\infty} \Big[\sum_{n=-\infty}^{\infty} \frac{1}{W_i}\, g(t, \tfrac{n}{W_i})\, W_i \cdot \exp[j2\pi f_i(\xi - \tfrac{n}{W_i}] \times \text{Sinc}[W_i(\xi - \tfrac{n}{W_i}] \cdot z(t-\xi)]\, d\xi$$

$$= \sum_{n=-\infty}^{\infty} g_n(t) \int_{-\infty}^{\infty} [z(t-\xi) W_i \cdot \exp[j2\pi f_i(\xi - \tfrac{n}{W_i})] \cdot \text{Sinc}[W_i(\xi - \tfrac{n}{W_i})]]\, d\xi \tag{2.12}$$

where $g_n(t) = \frac{1}{W_i}\, g(t, \frac{n}{W_i})$

The convolution of the input with the time function

$$W_i \exp[j2\pi f_i(t-n/W_i)] \text{ Sinc } W_i(t-n/W_i)]$$

corresponds to passing the input signal through a band-limited filter [4],

$$\text{rect}[(f-f_i)/W_i] \exp[-j2\pi nf/W_i)$$

For the case of WSSUS channel with input frequency constraints, the input band limiting filter can be incorporated

into the taps, with the result that the correlation properties can be shown to be [3]

$$\langle g_a^*(t)\, g_m(t+\tau)\rangle$$

$$= \int \exp[j2\pi f_i \tfrac{n-m}{W_i}]\ \mathrm{Sinc}[W_i(\xi - \tfrac{n}{W_i})]\cdot\mathrm{Sinc}[W_i(\xi - \tfrac{m}{W_i})]Q(\tau,\xi)d\xi \qquad (2.13)$$

where $Q(\tau,\xi)$ is as defined earlier.

If $Q(\tau,\xi)$ changes little for changes in ξ in the order of $1/W$, we have the approximation

$$\langle g_n^*(t)\, g_m(t+\tau)\rangle = \begin{cases} 0 & m \neq n \\ \frac{1}{W_i} Q(\tau, \frac{n}{W_i}) & m = n \end{cases} \qquad (2.14)$$

Thus the tap gains are uncorrelated random variables whose variance are proportional to $Q(n/W_i)$, the delay power density spectrum at the time n/W_i. Figure 2.1 shows the tapped delay line model.

2.5 Calculation of the Delay Power Spectrum [2]

Figure 2.2 gives the geometry for calculation of delay power spectrum. The details are as under :

r = height of transmitting antenna above the sea level

s = height of receiving antenna above sea level

d = straight line distance between transmitter and receiver

R_o = radius of earth to sea level

ψ_o = angle the radio horizon at the transmitter makes with the line connecting the transmitter and the receiver

ϕ_o = angle the radio horizon at the receiver makes with the line connecting the transmitter and the receiver

R = distance from the transmitter to differential scattering volume

S = distance from the receiver to the differential scattering volume dV

ψ = angle between R and D

ϕ = angle between S and D

θ = scattering angle i.e. angle through which incoming wave must be turned to scatter towards the receiver

h = height of volume dV above line connecting transmitter and receiver

c = velocity of light

Using the bistatic radar equation

$$dP \simeq \frac{GHdV}{R^2 S^2 h \theta_m} \qquad (2.15)$$

Bello has derived in [2] that

$$Q(\delta) \simeq \frac{1}{\delta^{1+m/2}} \int_{\psi_o/\sqrt{2\delta}}^{\sqrt{2\delta}/\phi_o} \frac{G(x\sqrt{2\delta} - \psi_o)\, H(\sqrt{2\delta}/x - \phi_o)}{(x + 1/x)^{m-2}\, x}\, dx \quad (2.16)$$

where the normalized path delay

$$\delta = \frac{\xi - D/C}{D/C},$$

ξ = path delay corresponding to differential scattering volume $= \frac{R + S}{c}$, and

x = a normalized variable = $\psi/\sqrt{2\delta}$,

m = scattering angle exponent.

For a Gaussian antenna patterns we have

$$G(\psi) = H(\psi) = \exp(-\psi^2/\sigma^2) \quad (2.17)$$

where σ may be expressed in terms of the half-power bandwidth of the antenna $\psi_{\frac{1}{2}}$, as

$$\sigma = 0.6\,\psi_{\frac{1}{2}} \quad (2.18)$$

and $$\psi_1 = \phi_o = D/2R_o \quad (2.19)$$

2.6 Parameters Used for the Simulation

The simulation was conducted using the following parameters :

Distance between the transmitter and receiver = 175 miles

Antenna diameter = 28 feet

Half power beam width of the antenna = 3 degrees

IF Bandwidth frequency = 70 MHz

RF Bandwidth = 12 MHz

Delay power spectrum time = .6 μsec

Number of mark space pairs

Type - I = 1

Type - II = 2

Type - III = 1

Pulse width

Type - I = .667 μsec

Type - II = 1 μsec

Type - III = 1 μsec

Number of taps on tapped delay line = 25

A sampling frequency of 40 MHz was used for generating the tapped delay line channel.

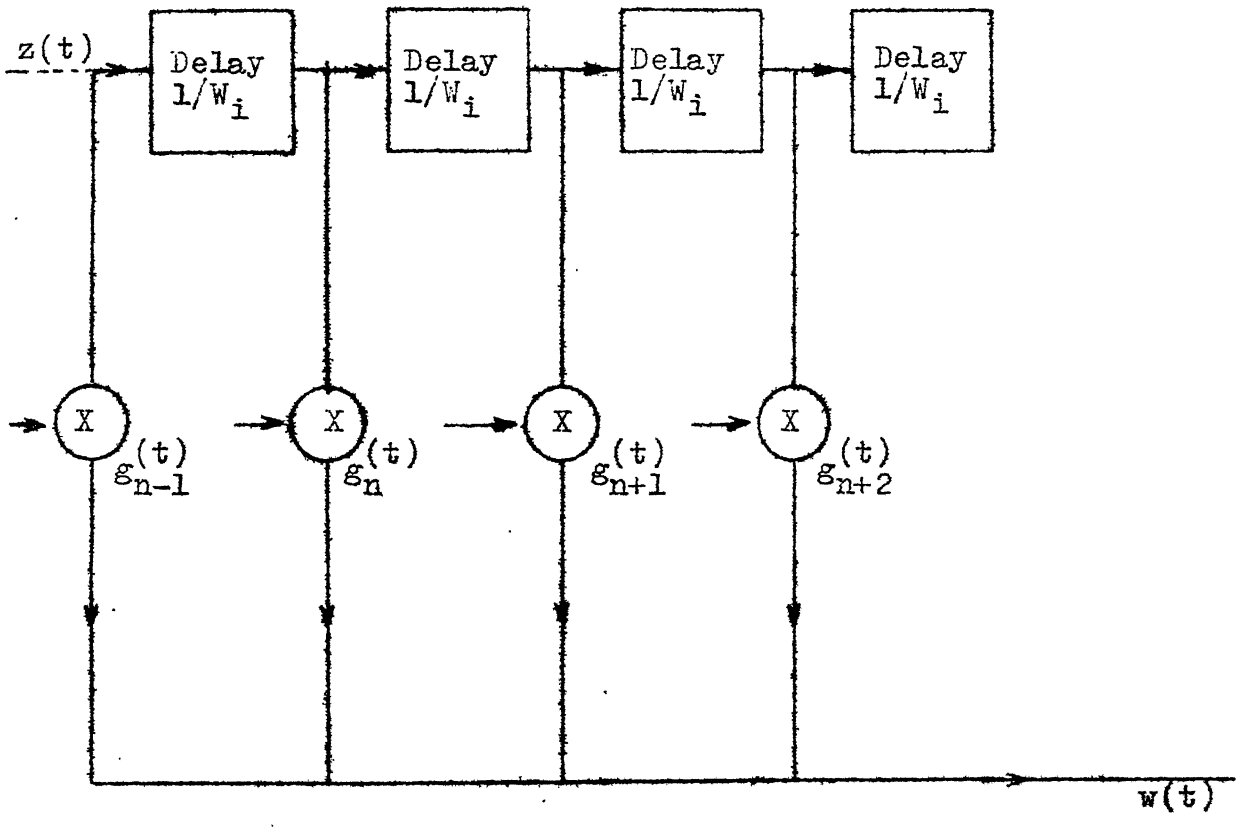

Fig. 2.1 The Tapped Delay Line Model

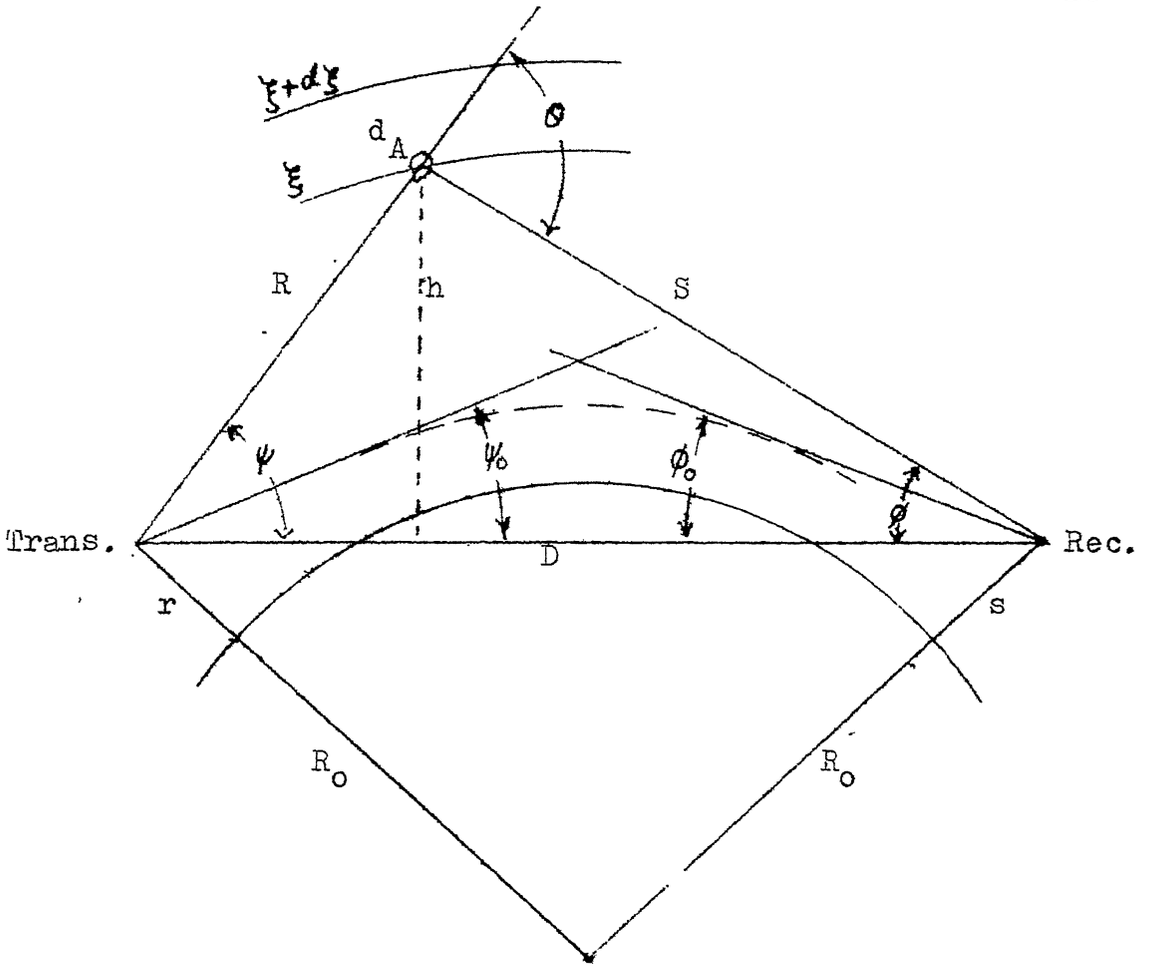

Fig. 2.2 Geometry for calculation of delay power spectrum

CHAPTER 3

DIGITAL FILTERING AND PSEUDO RANDOM NOISE GENERATION

3.1 Introduction

Digital filtering is the process of spectrum shaping. Even though the purpose of digital filtering is the same as that of analog filtering, the realization of a digital filter is quite different from that of an analog filter. Theory of analog filters is based on mathematics of linear differential equations while digital filtering is based on linear difference equations.

3.2 Design of Digital Filters

Digital filters can be designed by various techniques some of which are

a) impulse invariant method

b) bilinear transformation

3.2.1 The Impulse Invariance Method

The impulse response k(t) of a continuous filter is defined as the inverse Laplace transform of its system function Y(s).

$$k(t) = L^{-1}[Y(s)]$$

Similarly the impulse response h(nt) of a digital filter is defined as the inverse Z transform of its system function H(z).

Thus the condition that the impulse response of the digital filter is equal to the sampled impulse response of a continuous filter

$$L(nt) = k(t) \qquad t = 0,T,2T \ldots\ldots$$

L leads us to a digital filter.

3.2.2 Bilinear Transformation Method

If we have a stable analog filter defined by H(s), the frequency response of this filter can be found by evaluating H(s) at points on the imaginary axis of the s plane. Now if we have s replaced by a function of Z such that the imaginary axis of s maps onto the unit circle, then the resulting H(z) evaluated on the unit circle will take the same values that H(s) takes on the imaginary axis. The simplest rational function that maps the jw axis onto the unit circle is

$$s \longrightarrow \frac{Z - 1}{Z + 1} \tag{3.1}$$

3.3 Butterworth Filters

The class of analog filters with the system function

$$Y(s) = \frac{1}{\prod_{i=1}^{m} (s+s_i)} \tag{3.2}$$

having m poles at finite values of s and a m^{th} order zero for infinite s are called Butterworth filters.

A third order Butterworth Low pass analog filter has a system function [6]

$$Y(s) = \frac{s_1 s_2 s_3}{(s+s_1)(s+s_2)(s+s_3)} \qquad (3.3)$$

with $s_1 = w_c$,

$s_2 = \frac{1}{2}(1+j\sqrt{3})w_c$,

$s_3 = \frac{1}{2}(1-j\sqrt{3})w_c$

where w_c is the cut-off frequency, defined by $Y(jw_c) = 0.707$.

The Z transform of such a filter is

$$H(z) = \frac{CZ^{-1} + DZ^{-2}}{(1-e^{-w_cT}Z^{-1})(1-2e^{-w_cT/2}(\cos\frac{\sqrt{3}}{2} w_cT)Z^{-1} + e^{-w_cT}Z^{-2})} \qquad (3.4)$$

with

$$C = w_c\,[e^{-w_cT} + e^{-w_cT/2}(\frac{1}{\sqrt{3}} \sin\frac{\sqrt{3}}{2} w_cT - \cos\frac{\sqrt{3}}{2} w_cT)]$$

and

$$D = w_c[e^{-w_cT} - e^{-3w_cT/2}(\frac{1}{\sqrt{3}} \sin\frac{\sqrt{3}}{2} w_cT + \cos\frac{\sqrt{3}}{2} w_cT)]$$

3.4 Design of Complex Digital Filter [7]

Consider a bandpass function centered around w_c. The real part r(t) can be defined as

$$r(t) = \text{Re}\,[z(t)]$$

$$= \text{Re}\,[e(t)e^{jw_c t}]$$

$$= \text{Re}\,[e(t)\ \text{Cos}\ w_c t - \text{Im}[e(t)]\ \text{Sin}\ w_c t \qquad (3.5)$$

This is a compact representation of the in phase and quadrature components of the bandpass function. The effect of the modulation by $e^{jw_c t}$ is merely a translation of the spectrum by an amount w_c.

Hence, in developing a complex filter we start with a real filter centred around $w = 0$ and shift the centre point so that the desired amplitude and phase are now obtained relative to a new frequency w_c, without introducing a conjugate filter at $-w_c$, as would have occured in the case of a lowpass to bandpass transformation in a real filter.

Mathematically this shift is accomplished by replacing s by $s - jw_c$ in the real filter transfer function H(s). This is equivalent to multiplying the impulse response by $e^{jw_c t}$. The mapping

$$Z = e^{st} \qquad (3.6)$$

accomplishes this s plane transfer along jw axis. to a z plane shift for the digital filter [7].

Hence, we get

$$Z_{\text{shifted}} = e^{(s - jw_c T)} = e^{-jw_c T} Z \qquad (3.7)$$

Hence if we define $\gamma = e^{-jw_c T}$,

$$Z_{shifted} = \gamma Z \tag{3.8}$$

The result of this transformation is that the poles/zeros are rotated by $w_c T$ radians from its previous location.

If we now have the filter system function using the delay operator Z^{-1} as

$$H(z^{-1}) = \frac{C_o + C_1 Z^{-1} + \ldots\ldots + C_p Z^{-p}}{D_o + D_1 Z^{-1} + \ldots\ldots + D_q Z^{-q}} \tag{3.9}$$

the recursive relationship to implement this being

$$y_m = - \sum_{i=1}^{q} d_i \, y_{m-i} + \frac{1}{d_o} \sum_{j=0}^{p} c_p \, x_{m-j} \tag{3.10}$$

where $[x_i]$ and $[y_i]$ are the filter inputs and outputs respectively, the conversion to a complex filter involves using new coefficients c_{ls} and d_{ls} such that [7]

$$c_{ls} = \gamma^{-1} \, c_l \quad \text{and} \tag{3.11}$$

$$d_{ls} = \gamma^{-1} \, dl \tag{3.12}$$

This can be implemented recursively on a digital computer. Therefore, the design of a complex digital filter involves

a) Design of a lowpass digital filter

b) Shifting the filter characteristics to bandpass characteristics at the desired frequency.

3.5 Details of Filters Designed

A bank of IF filters were used in the simulation. The IF frequency was 70 MHz and the RF bandwidth was 12 MHz. We designed for Frequency Diversity Type I four third order Butterworth bandpass filters each having a bandwidth of 3 MHz as per details given in Sections 3.3 and 3.4. The lower two frequencies were assigned to mark and the upper two for space. The highest frequency to be passed being 76 MHz, we had a sampling frequency of 152 MHz.

For the study of frequency diversity Type II and Type III since we required a bank of six IF filters in the assigned bandwidth of 12 MHz, we had to design new filters each with a passband of 2 MHz, centred at 65 MHz, 67 MHz, 69 MHz, 71 MHz, 73 73 MHz, and 75 MHz. These were also third order Butterworth filters. The filters having centre frequencies of 65 MHz and 75 MHz were assigned as diversity frequencies. The remaining four were assigned so that the lower two frequencies were meant for mark and the upper two frequencies were for space.

3.6 Pseudo Random Noise Generator

In this simulation, complex Gaussian noise had to be added to the signal. The generation of complex Gaussian noise was done by generating pseudo random numbers which are uniformly distributed and then using a transformation to obtain a Gaussian distribution.

3.7 Generation of Uniform Distribution

The library subroutine for generation of pseudo random numbers uses the multiplicative congruential method. It consists of computing i +1th random number using the relationship,

$$x_{i+1} = x_i \times a \text{ (modulo m)} \qquad (3.13)$$

where x_i = ith pseudo random number, and

a = a constant multiplier.

The library subroutine has a fixed starting seed. Therefore, the sequence of random numbers generated were the same for each simulation run since each simulation started with the same seed. Since the time for a single run was limited it was not possible to generate a continuous long sequence of random numbers.

Since there was no provision for seeding the library subprogram for each run, it could not be used in this simulation. It was therefore essential to write a seperate function subprogram which could return the seed for subsequent iterations at the end of each run. Using these seeds as the starting seeds for the subsequent run, it was possible to generate suitable lengths of signal sequences without losing the generality of the entire sequence.

3.8 Generation of Gaussian Distribution

The Gaussian distribution was generated using the Box - Muller transformation

$$s = (-2 \log_e r_1)^{\frac{1}{2}} \cos(2\pi r_2) \qquad (3.14)$$

where r_1 and r_2 are two uniform random numbers between 0 and 1 and s is the desired normal distribution.

To generate Gaussian distribution with a specified mean and variance, we use the relationship

$$x = \sigma s + \mu \qquad (3.15)$$

where x is the sample from a normal distribution with specified mean μ and variance σ. s is as per eqn. (3.14).

Since in this simulation we have to generate a complex Gaussian number, we generate two independent and identically distributed Gaussian numbers X and Y by eqns. (3.14) and (3.15) and form the complex sample Z as given below

$$Z = X + jY \qquad (3.16).$$

CHAPTER 4

SYSTEM DESCRIPTION AND DIVERSITY

4.1 Signal Flow Model

The energy detection FSK system as given in [3] has been used for this study. Fig. 4.1 shows the simplified block schematic of such a system.

In the actual system the modulated carrier through the channel tis passed through a demodulator. The output of the demodulator is fed through mark and space IF filters and then a decision is taken based upon which is the larger output.

4.2 Simulated System

The signal flow diagram used in the simulated system is shown in Fig. 4.2.

In the case of the simulated system, we first form the channel using the tapped delay line model [1], [3]. The sign sequence generator generates the signal deciding a mark or a space based upon a uniform distribution. The frequency to be transmitted is chosen based upon firstly whether it is a mark or space and secondly the time slot in which it is to be transmitted. The signalling schemes that were used for various diversities are described later in this chapter.

4.3 Channel Formulation

The total number of taps required in the delay line is

calculated as follows :

$$\text{M TAPS} = \frac{\xi_{max} - \xi_{min}}{1/W_i}$$

$$= W_i(\xi_{max} - \xi_{min})$$

$$= W_i \Delta \qquad (4.1)$$

where

Δ = Multipath delay

ξ_{max} = Maximum path delay

ξ_{min} = Minimum path delay

W_i = Sampling frequency

The delay power spectrum $Q(\delta)$ was computed by evaluating the integral in eqn. (2.16) mentioned in Chapter 2 for various values of δ. The delay power spectrum is then sampled MTAPS times. These MTAPS values of $Q(\delta)$ are previously calculated and stored in the computer prior to the simulation. The complex tap gains g_n are found by using these MTAPS samples of the delay power spectrum $Q(\delta)$ in the relationship

$$g_n = (a_n + jb_n)\sqrt{\frac{Q(0,n/W) * \text{DNSMPL}}{2W}}$$

$$1 \leq n \leq \text{MTAPS}$$

where a_n and b_n are Gaussian random variables of zero mean and unity variance, DNSMPL = the downsampling factor, and

W = the sampling frequency.

4.4 Modulation

In the modulator based upon the frequency, the signal is convolved with the channel using a recursive digital filtering technique described in [3]. We use the relationship

$$x_n = y_n + e^{jwT} x_{n-1} - e^{jmwT} y_{n-m} \qquad (4.3)$$

where the $[y_i]$ are sampled unit pulses, then the resulting $[x_i]$ will be equal to

$$x_i(nt) = \begin{cases} e^{jwnT}, & 0 \leqslant n \leqslant M-1 \\ 0, & n \geqslant M \end{cases} \qquad (4.4)$$

Thus we generate a M sample burst of a complex exponential with an angular frequency w. If now an arbitrary sampled sequence $[y_i]$ is used as the input to eqn. (4.3) the resulting output will be the convolution of $[y_i]$ with the filter.

FSK signals are rectangular bursts of complex exponentials. Therefore, if we use the complex tap gains of the channel as the set $[y_i]$ in eqn. (4.3) where w is the angular frequency of the FSK burst, then the output of the channel is the set $[x_i]$ as shown in eqn. (4.4). This relationship eqn. (4.3) is the shortest means for finding the effects of the channel on the signal and can be, for long channels, orders of magnitude faster than the usually used time domain convolution [3].

4.5 Digital Filter

The output of the modulator is now fed to digital IF filters for the mark and space frequencies. These are third order Butterworth filters. These filters are complex, digital filters having a passband of width W about some desired frequency Ω. Unlike real filters, complex filters do not have passband centered around $-\Omega$.

These filters were designed using techniques given in [6], [7]. The details of the digital filters design has already been given in Section 3.5.

4.6 Gaussian Noise Generation

Complex Gaussian Noise of zero mean and unity variance is generated as described earlier in Section 3.8. This noise is filtered through the respective IF filters and then is added to the signal after giving it necessary weightage to maintain a particular SNR.

4.7 Energy Calculation

The energy in the signal and noise, and the noise only are computed separately by summing the energy in the signal plus noise sequences and the noise sequences. This is done by summing the square of the magnitude of each sample.

4.8 Decision

A decision is arrived at this stage whether an error has

occured or not. This is done on the basis of comparing the energy contained in osignal plus noise with the energy contained in only noise. An error has occured when the energy in noise filter is greater than the energy in the message carrying filter. Only under such circumstances, do we refer to the diversity channels, i.e. In case of a correct decision in the first channel we do not consider the energy of the diversity channel.

4.9 Computation of Statistics

On completion of a every 100 samples the number of errors that would have occured is printed out. This data is logged for each SNR so that the total number of errors can be computed for each SNR. Along with this the number of times the diversity channel was considered is also printed out.

4.10 Diversity

The aim of the simulation was to study the implicit diversity in the received waveform by virtue of frequency selective fading imposed by the channel on the received signal.

4.11 Diversity Combining

The optimal method of combining the diversity is predetection maximal ratio combining [4], which involves

weighting each diversity channel received signal, by a complex gain which is proportional to the conjugate of the channel gain and inversely proportional to the noise. However, in the case of this study due to paucity of computer time, we have used a modified form of equal gain post detection combining. In this case, we have referred to the diversity channel only in the case of an error. That is, if the first channel gives an error we refer to the diversity channel and sum up the energy of the signal and noise of the diversity channel and the first channel before arriving at a decision.

Thus, if

$$\sum_{k=1}^{k}\left[\sum_{i=0}^{M-1}(s_i(t)+n_i(t))^2-\sum_{i=0}^{M-1}(n_i(t))^2\right]<0 \qquad (4.5)$$

where

s(t) = signal amplitude

n(t) = noise amplitude

k = order of diversity

M = number of samples per gate time,

an error occurs.

In our case, to reduce computer time we take a decision for k = 1 and in case of an error go for higher orders of diversity.

4.12 Signalling Scheme

The total allowable RF bandwidth is divided into two equal, adjacent, non overlapping frequencies called the

'Mark' and 'space' bands. Each Mark and Space division is further divided into N equal divisions each numbered from 1 to N in each band.

The FSK transmission utilized to transmit at time t_I, $1 \leqslant I \leqslant N$, a gated sine wave at either frequency M(I) or S(I) based upon whether a mark or a space is required to be transmitted. In the case of diversity transmission, signal formats as shown later in this chapter were transmitted. The pulse width T for the system is a constant. Also,

$$T \leqslant t_{I+1} - t_I \tag{4.6}$$

Also, if the multipath spread is to be limited to δ seconds,

$$N(t_{I+1} - t_I) \geqslant \delta \tag{4.7}$$

If B_{max} is the maximum allowable bandwidth and W is the bandwidth of the pulse then,

$$2\,NW \leqslant B_{max} \tag{4.8}$$

4.13 Signal Format Used

Three types of signalling formats were used. Each one consisted of a frequency time pattern. These are dealt with in detail below.

4.13.1 Frequency Diversity Type I

Figure 4.3 illustrates the frequency diversity Type I.

The bandwidth allocation here being 4 W_o, we send the lower two frequency bands for Mark and the upper two frequency bands for space. Hence let us say a Mark occurs then we send f_1 in time slot t_1 and the diversity channel is f_2 in time slot t_2. Similarly, for Space we send f_3 in time slot t_1 and f_4 in time slot t_2. The data rate in this case is $\frac{1}{2T}$ b/secs with a bandwidth occupancy of 4 W_o. If we assume w_o as W, the data rate packing is $\frac{1}{8TW}$ bits/sec/Hz.

In detection, time gates of duration $T_o = 2T$ are applied after the appropriate bandpass filters. Computation of the energy in the gated waveform provides the decision variables. Thus for the Mark filter time gate output would contain signal plus noise

$$W_m(t) = S(t) + n(t)$$

While the Space filter would contain only noise

$$W_s(t) = n(t).$$

Thus an error would occur if

$$\sum_{i=0}^{M-1} \left| S_i(t) + n_i(t) \right|^2 - \sum_{i=0}^{M-1} \left| n_i(t) \right|^2 < 0 \qquad (4.9)$$

In the case of Type I, since we have a kind of second order diversity, the decision is taken after considering both the channels. Thus an error occurs if

$$\sum_{k=1}^{2} \left[\sum_{i=0}^{M-1} \left| S_i(t) + n_i(t) \right|^2 - \sum_{i=0}^{M-1} \left| n_i(t) \right|^2 \right] < 0$$

4.13.2 Frequency Diversity Type II

Figure 4.4 illustrates the signalling format used in the diversity type II.

In this case, we have two diversity channels at either end of the allocated bandwidth. The rest of the bandwidth is divided into four bands, the lower two frequency bands like earlier are for the mark and the upper two for the space frequencies. The diversity channel is chosen as the basis of whether a mark or space is sent and the time slot in which it is sent. For example, if a mark is sent in time slot t_1, the diversity channel is f_1. So, the frequencies transmitted are f_2 and f_6. Similarly, in time slot t_2 the frequencies are f_1 and f_3 for mark. In the case of space, in time slot t_1 the frequencies sent are f_4 and f_6 and in time slot t_2, the frequencies are f_5 and f_1.

The channel being the same for both the main channel and the diversity channel, the noise is constant during a time slot .

Thus, for a mark in time slot t_1, we sum up the energy in mark filter f_2 and diversity filter f_6 and compare it with the sum of the two noise energies in the respective space filters.

Like earlier, an error occurs if

$$\sum_{k=1}^{2}\left[\sum_{i=0}^{M-1}\left|S_i(t)+n_i(t)\right|^2-\sum_{i=0}^{M-1}\left|n_i(t)\right|^2\right]<0 \qquad (4.11)$$

The data rate in this case is 1/T bits per second with a bandwidth allocation of 6 W_o. Again, assuming W_o as W the data rate packing factor in this case is $\frac{1}{6TW}$ bits/sec/Hz.

4.13.3 Frequency Diversity Type - III

In this case the signal format used is as shown in Fig. 4.5.

This is similar to the frequency diversity case with the essential difference being that two time slots are used for each signal. Here, if say a Mark occurs, we transmit frequencies f_2 and f_6 in time slot t_1, f_3 and f_1 in time slot t_2. In the case of space, the frequencies are f_4 and f_6 in time slot t_1 and f_1 and f_5 in time slot t_2.

An error occurs in this case if

$$\sum_{k=1}^{4}\left[\sum_{i=0}^{M-1}\left|S_i(t)+n_i(t)\right|^2-\sum_{i=0}^{M-1}\left|n_i(t)\right|^2\right]<0 \qquad (4.12)$$

The data rate in this case is 1/2T bits per second, with a bandwidth allocation of 6 W_o. Again assuming W_o as W, the data rate packing factor in this case is 1/12TW bits/sec/Hz.

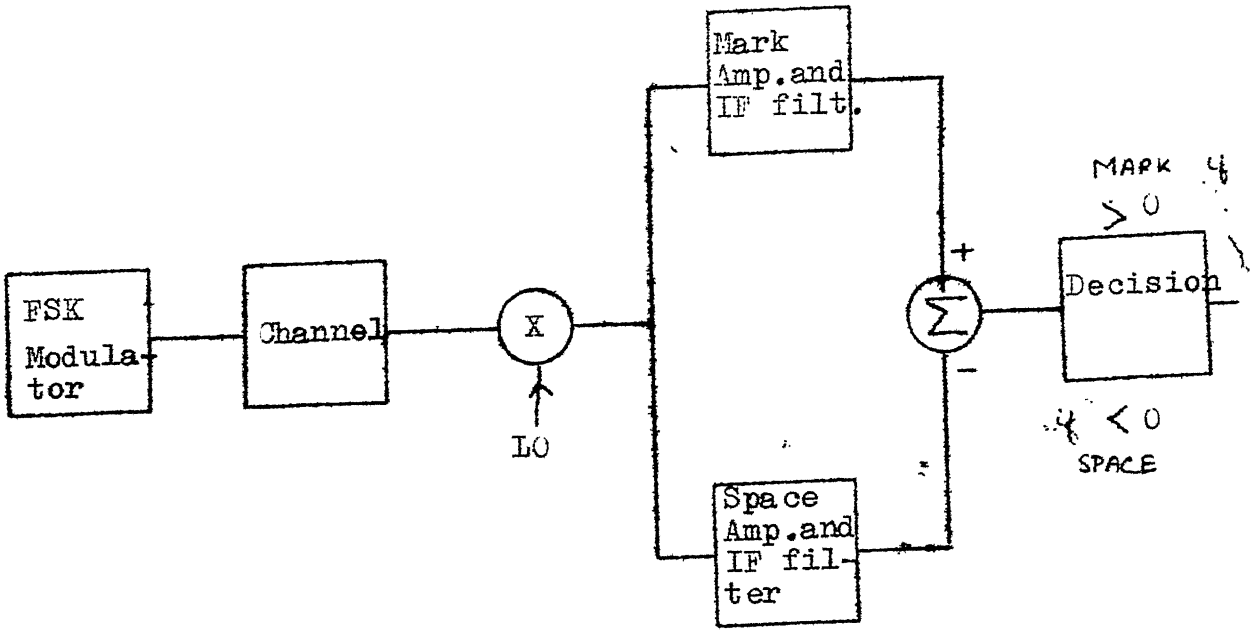

Fig. 4.1 Signal Flow Diagram

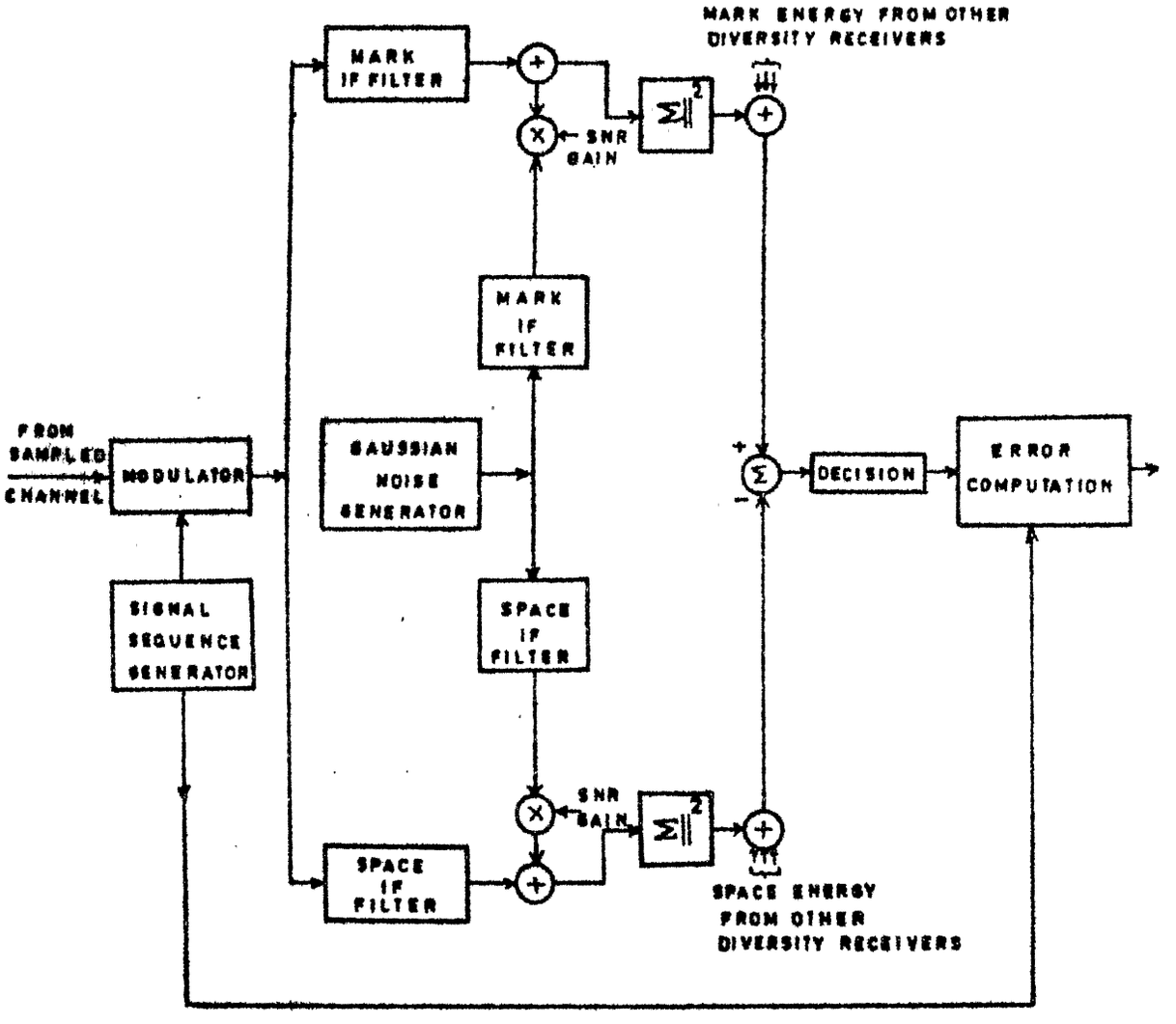

FIG.4.2 SIGNAL FLOW DIAGRAM OF SIMULATED SYSTEM

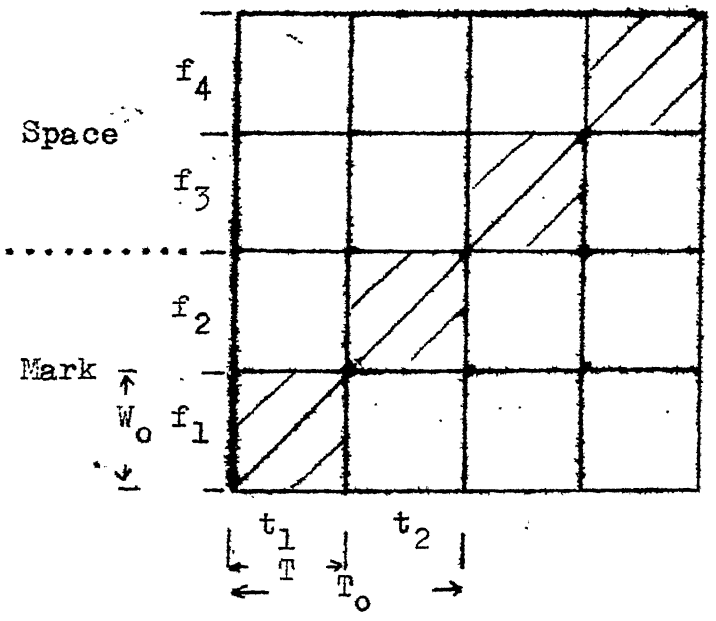

Fig. 4.3 Signalling Format Type I

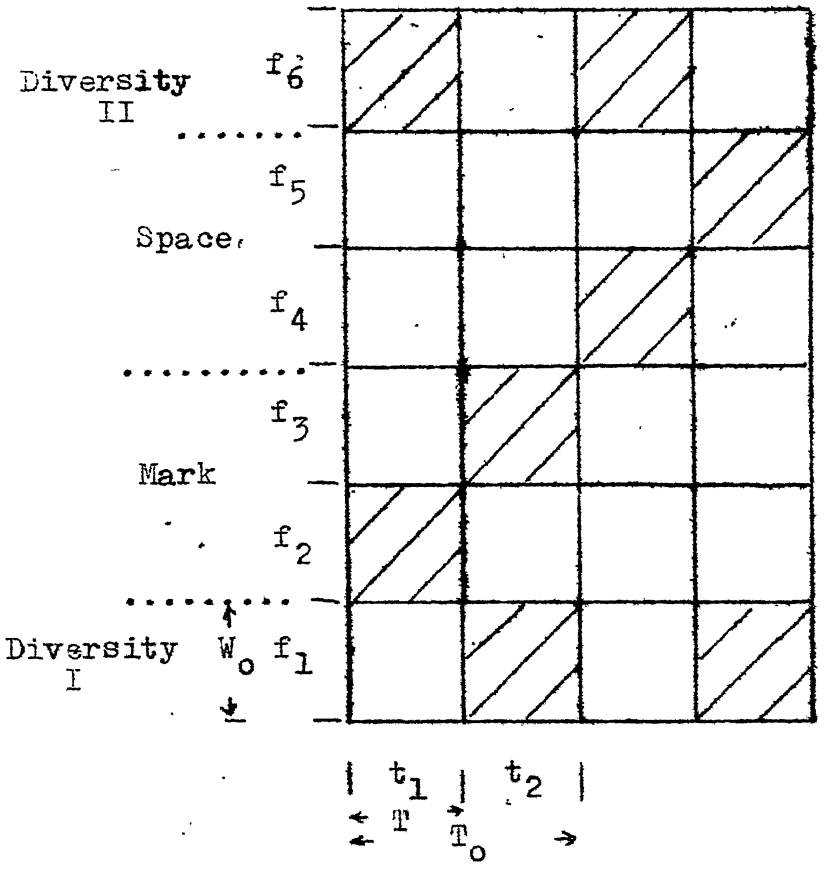

Fig. 4.4 Signalling Format Type II

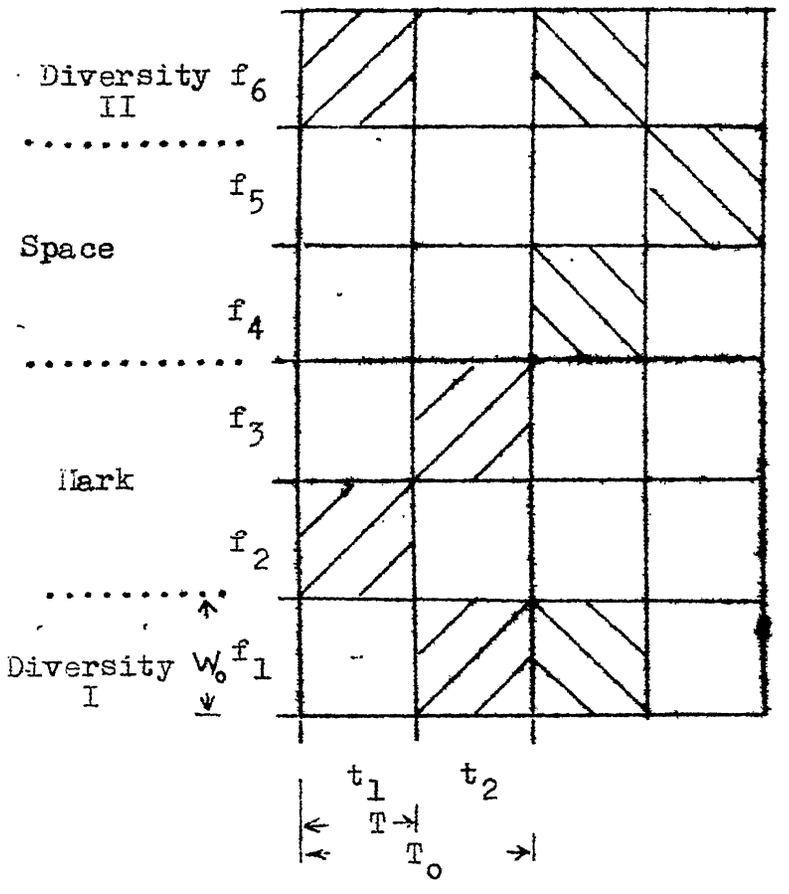

Fig. 4.5 Signalling Format Type III

CHAPTER 5

SIMULATION AND RESULTS

5.1 Introduction

All the parameters for the simulation have been taken from proposed or existing mobile troposcatter systems. A Fortran program for the event to event simulation of the system was written. The program is modular in construction with the main program controlling all the subroutines. The system was simulated on the Digital Computer IBM 7044.

5.2 Main Program

The flow chart of the main program is given in Fig. 5.1. The details are as under :

Block 'A' : The seeds for the generation of the uniform random numbers for deciding mark/space and generating a Gaussian distribution is read in as data. The weights for realizing the various signal-to-noise ratios is also fed in here. The centre frequencies for the various IF filters is also an input parameter. The total number of samples for each computer run NSAMP and the SNRs for which the simulation is done is also decided.

Block 'B' : In this block the various counters/flags that are required for computing various statistics at the end of a simulation are initialized. These are for counting :

(a) Number of signal samples i.e. mark/space

(b) Number of errors

The total energy in signal plus noise and the total energy in noise alone are also initialized to zero here, so as to evaluate the SNR. The various flags that are required during the simulation run are also initialized here.

Block 'C' : In this block the various storage locations that require initializing for each iteration are initialized. These include :

(a) Signal plus noise energy of each signal sample

(b) Noise energy of each signal sample

(c) Flag to decide signal sequence and frequency to be transmitted which is dependent upon type of diversity considered.

(d) The iteration counter is incremented here

Block 'D' : In the block D1 it is decided whether the signal is a mark or a space based upon a uniform distribution. In the second part of this block D2 on the basis of the signal being a mark or a space, the time slot and the type of diversity being used, the signal pattern that has to be sent through the system is is formulated. The system patterns are given in Figs. 4.3, 4.4, 4.5

Block 'E' : The channel is formed by calling the subroutine CHANNEL. This consists of generating the 25 complex tap gains of the tapped delay.

Block 'F' : Digital filtering of the complex tap gains is done prior to convolving the channel in subroutine DIGIFL. The Digital filtering operation is done at the particular IF filter centre frequency which has been decided earlier. The bandwidth of the IF filter is 3 MHz in the Type I and 2 MHz in Type II and III.

Block 'G' : The signal is convolved with the filtered channel using subroutine CONVOL here using the algorithm mentioned in Section 4.4 described earlier in Chapter IV. We use 26 samples of complex exponential at the specified frequency which are convolved with the 25 complex tap gains of the tapped delay line. The output of the convolution is 50 samples of convolved frequency.

Block 'H' : Complex Noise is generated in this block using a subroutine NOIS that generates a complex Gaussian distributed number. These are then digitally filtered using subroutine DIGIFL.

Block 'J' : This block reduces the noise as per the SNR required for the simulation using a weighting factor.

Block 'K' : In subroutine ENERGY the suitably weighted fifty complex samples are individually added to the fifty complex noise samples. The energy of signal plus noise is computed. Similarly the energy of noise is computed. This is done by evaluating the square of the magnitude in each case and summing it over 50 samples in each gate time.

Block 'L' : It is decided at this stage whether the total energy of the fifty signal plus noise samples is greater than total energy of fifty noise samples alone.

Block 'M' : If in the first instance the signal plus noise energy is less than noise energy, the diversity channel is considered by branching to points 20,30 and 40,which are predecided depending on the signalling format for which the system is being tested. The main channel is first tested and if the signal plus noise energy is greater than noise energy alone we take it as a no error case and skip to the next sample.

An error occurs only when the total signal plus noise energy is less than the total noise energy for all diversity channels. This is a variation over the equal ratio post detection combining that should have been done in an actual system. This was done so as to reduce the computation time.

Block 'N' : On completion of the specified number of samples NSAMP, for the computer run, statistics are computed in this block. These statistics are :

(a) Total number of iterations, i.e. Number of signal samples for which the system was tested NSAMP

(b) Number of errors

(c) Number of times diversity channel was used

(d) Signal to noise ratio

5.3 Results

The system was simulated for signal-to-noise ratios (SNR) of 0,3,6,10,20,23 and 24.5 dB for types I and II. In Type III the signals-to-noise ratios for which the system was tested are as above except for 23 & 24.5 dB.The small signal-to-noise ratios of 0,3 and 6 dB were simulated with a runs of over 1000 samples for each SNR. The larger SNRs of 10,20,23 and 24.5 dB were tested with a simulation length of over 4000 samples.

The graph showing probability of error versus signal-to-noise ratio are shown in Fig. 5.2. The probability of error is better in all types of diversity than the 2 FSK case as simulated in [8].

It is found that Type I has a smaller probability of error as compared to Type II. This should be expected since the

bandwidth of the IF filters is just 2 MHz in Type II as compared to 3 MHz in Type I.

Frequency diversity Type III being a kind of quadruple diversity, it has the lowest probability of error. A comparison of data rates shows that the diversity Type II has a better data rate than I and III for the same bandwidth. Among the three cases it is seen that probability of error is least in Type III even though there is a reduction in data rate by half as compared to Type II using the same bandwidth.

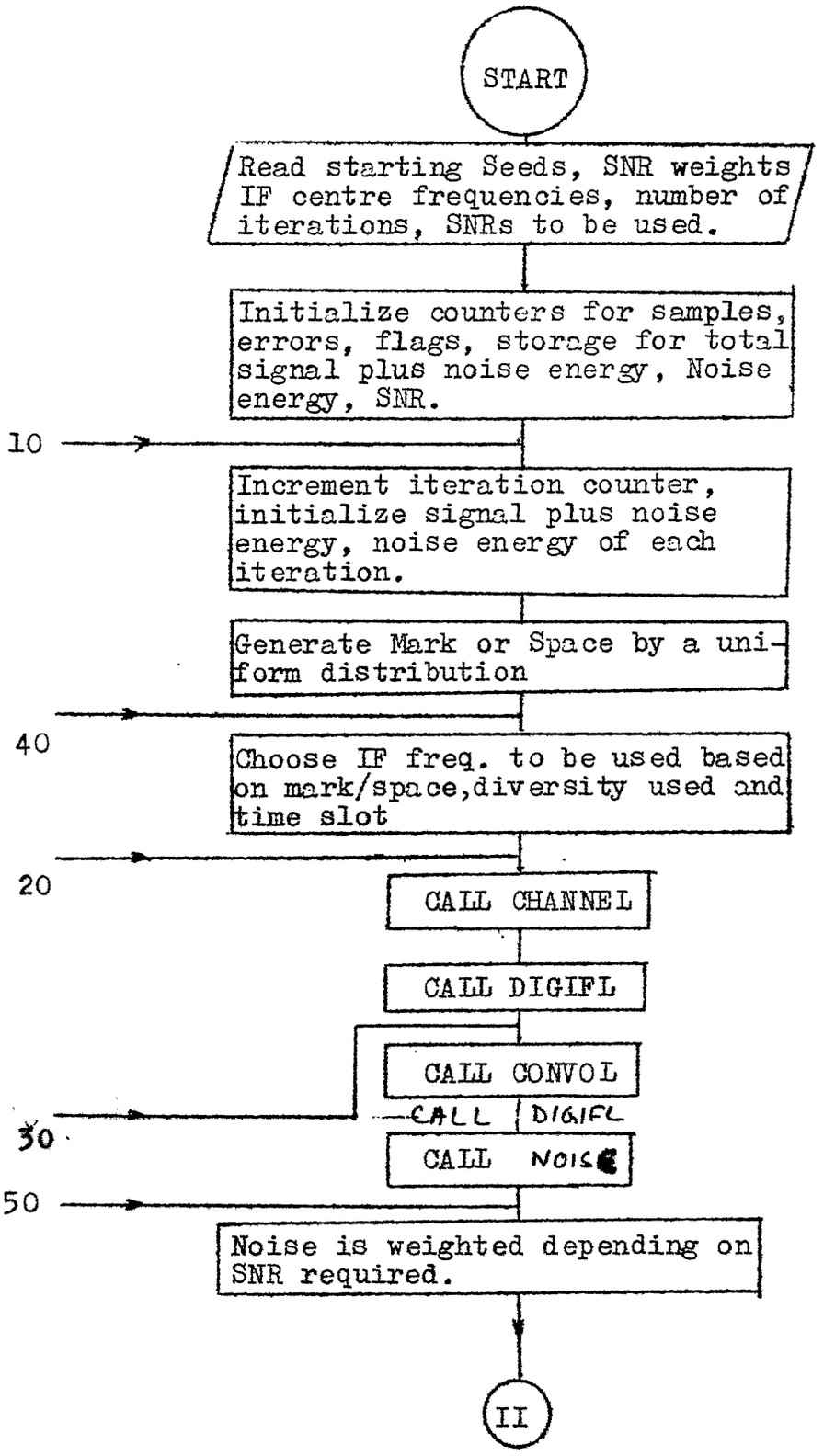

Fig. 5.1 Flow Chart

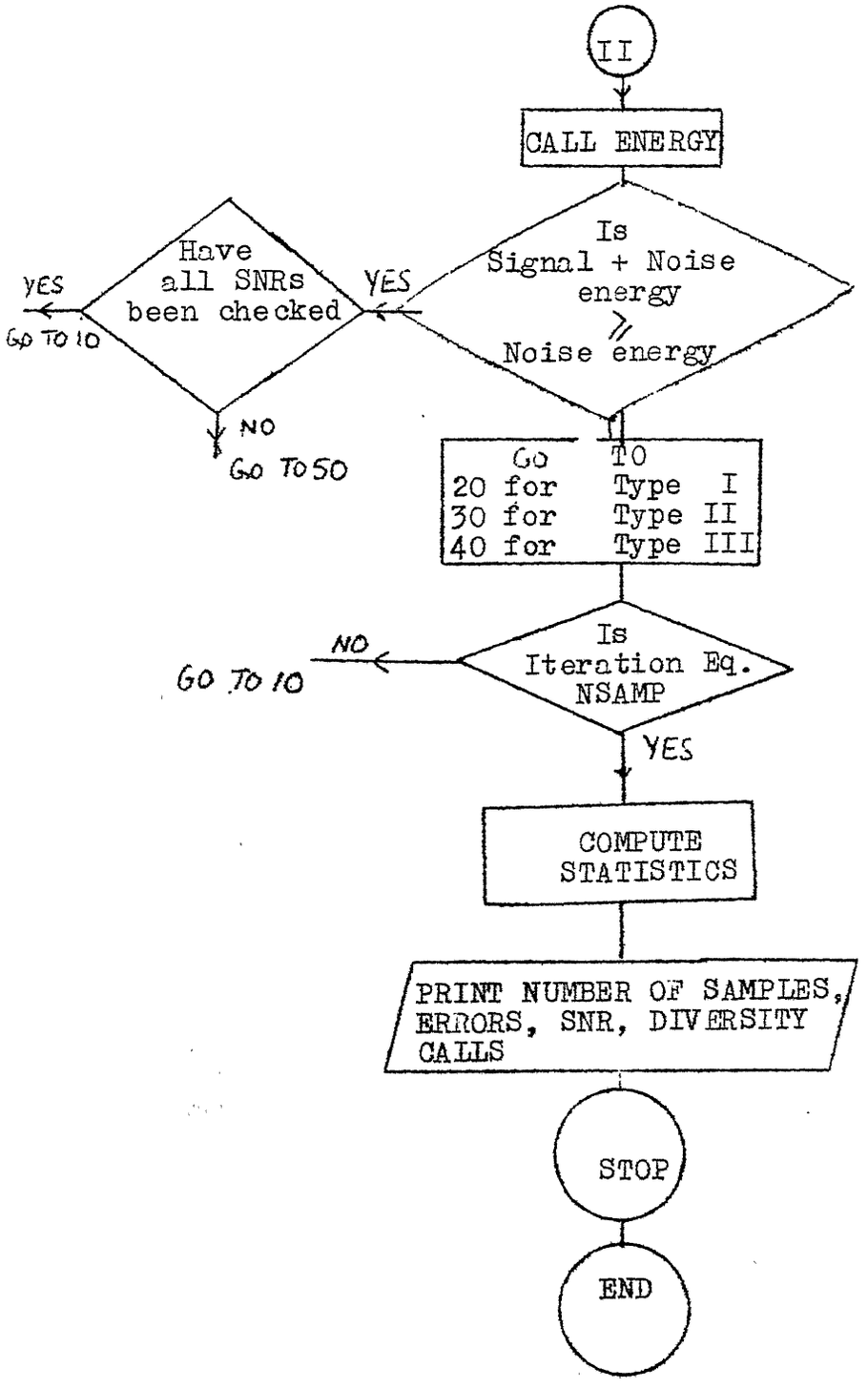
II
CALL ENERGY
Is
Signal + Noise
energy
≥
Noise energy
YES
Have
all SNRs
been checked
YES
GO TO 10
NO
GO TO 50
GO TO
20 for Type I
30 for Type II
40 for Type III
Is
Iteration Eq.
NSAMP
NO
GO TO 10
YES
COMPUTE
STATISTICS
PRINT NUMBER OF SAMPLES,
ERRORS, SNR, DIVERSITY
CALLS
STOP
END

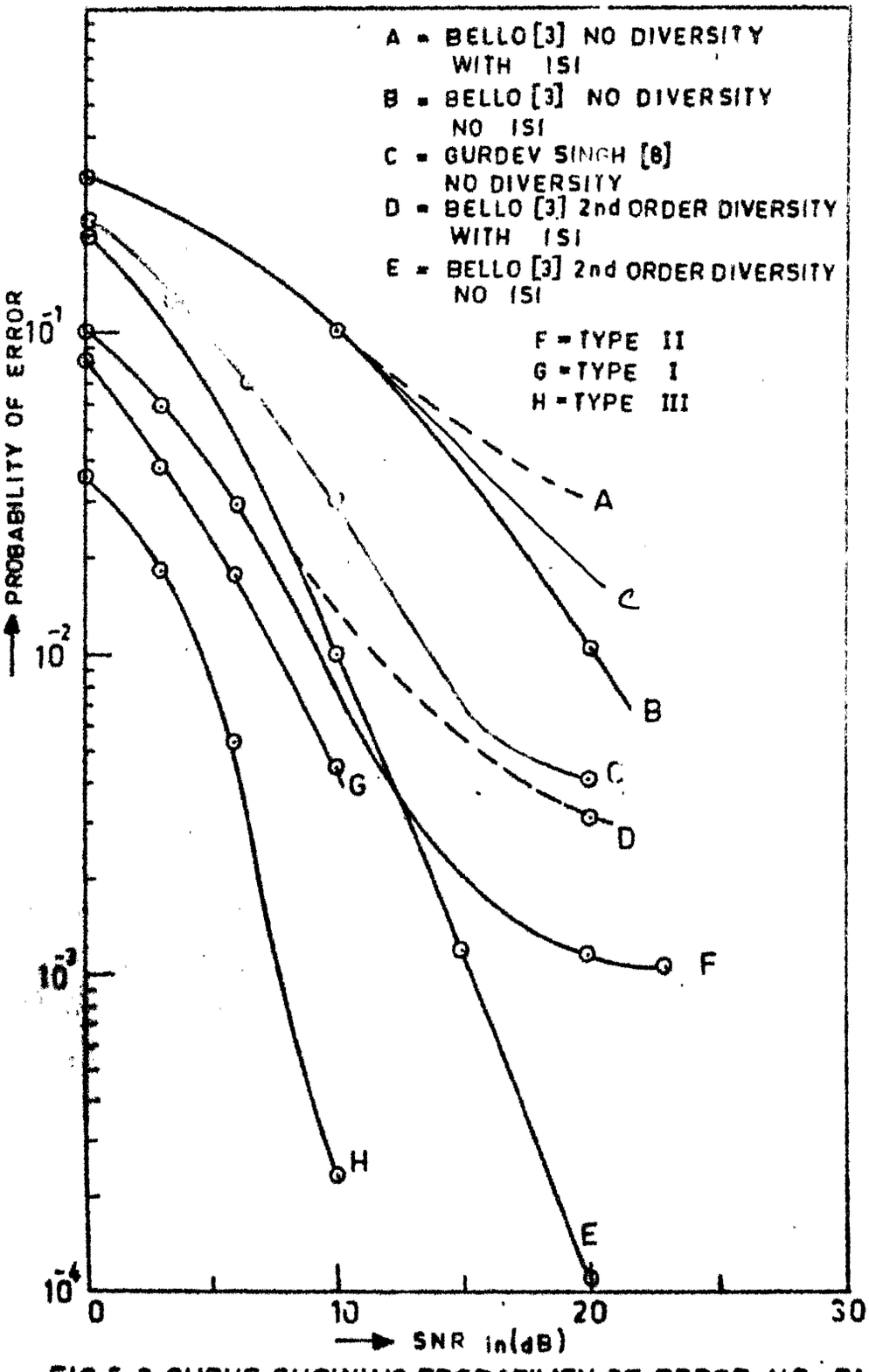

FIG.5.2 CURVE SHOWING PROBABILITY OF ERROR VS SNR

CHAPTER 6

CONCLUSION

In this thesis we have studied some techniques of inband diversity that would be suitable for a mobile troposcatter system. Incorporating such a technique of diversity in a system has the advantage of reduction of bulk that is essential for mobile troposcatter systems. The conventional forms of diversity like space and frequency do not permit such a drastic reduction in bulk though they do have better data rates. Inband frequency diversity also reduces alignment time as compared to conventional forms of diversity.

Simulation of a troposcatter system like in this case takes many hours of computation time on a fast digital computer. In this case at various stages we had to introduce modifications so as to reduce the computer time. With this in view, the type of combining had to be modified, so as to take a decision based on the main channel itself if correct and adding diversity channel energies only in the case of errors. This will give quite an optimistic estimation of the probability of error. Further, the simulation length had to be curtailed drastically due to prolonged computation time. It is necessary to have atleast eight to ten such simulation runs for each SNR before we can fix any probability of error with some degree of confidence.

The results obtained here give only an idea about the performance of the systems simulated but longer and more simulation runs are required to have a more accurate estimate of the probability of error. We expect better performance at higher SNRs while using inband frequency diversity. There is a drastic reduction in the data rate by these forms of diversity as compared to the conventional forms like frequency and space. A fourth order diversity scheme using a time frequency pattern like Type I involves reduction in the data rate to a quarter of the original data rate. However, with usage of codes as in Type III, it should be possible to increase this data rate so that we can still get a fourth order diversity with a reduction in data rate by only 0.5. Many such codes can be used for transmission of signals.

One such possibility is the usage of the signalling format shown in Fig. 6.1. This is another case of coded diversity. Here when a mark occurs, we transmit in time slot t_1 frequencies f_1 and f_4 and in time slot t_2 frequencies f_2 and f_3, whereas in the case of space we transmit frequencies f_2 and f_3 in time slot t_1 and frequencies f_1 and f_4 in time slot t_2. Since this requires only four bands, this has a higher data packing factor as compared to Type III mentioned earlier. It should also have a probability of error comparable to Type III.

One of the promising new areas of signal design for fading dispersive channels is the usage of error correction codes. D. Chase in [10] gives a combined coding and modulation approach for communication over such channels. It is intuitively possible to visualize that considerable performance improvements is possible with coding without any loss in data rate beyond the normal redundancy of the code.

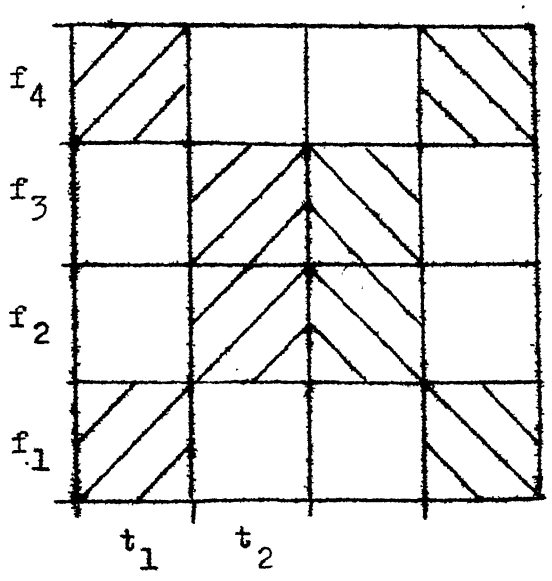

Fig. 6.1 A Signalling Format Possible

REFERENCES

[1] P.A. Bello, 'Characterization of random time-variant linear channels', IEEE Trans. on Communication Systems, Vol. CS-11, pp 360-393, December 1963.

[2] P.A. Bello, 'A Troposcatter channel model', IEEE Trans. on Communication Technology, Vol. COM-17, April 1969.

[3] P.A. Bello and L. Ehrman, 'Performance of an Energy Detection FSK Digital Modem for Troposcatter links', IEEE Trans. on Communication Technology, Vol. COM-17, No.3, pp 368-379, June 1969.

[4] M. Schwartz, W.R. Bennett and S. Stein, Communication Systems and Techniques, McGraw-Hill, New York, 1966.

[5] P.A. Bello, 'Aeronautical Channel Characterization', IEEE Trans. on Communication, pp 548-563, May 1973.

[6] C.M. Rader and B. Gold, 'Digital Filter Design Techniques in the Frequency-Domain', Proc. IEEE, Vol. 55, pp 149-171, February 1967.

[7] T. Crystal and L. Ehrman, 'The design and applications of digital filters with complex coefficients', IEEE Trans. Audio and Electroacoustics, Vol. AU-16, pp 315-320, September 1968.

[8] Gurudev Singh, 'Simulation of energy detection troposcatter system, M.Tech. Thesis, IIT Kanpur, 1978.

[9] P. Monsen, 'Performance of an experimental angle diversity troposcatter system', IEEE Trans. Communications, Vol. COM-20, pp 242-247, April 1976.

[10] D. Chase, 'A Combined Coding and Modulation Approach for Communications Over Dispersive Channels', IEEE Trans. on Communications, March 1973.

[11] P.A. Bello, 'Selection of Multichannel Digital Data Systems',for Troposcatter Channels', IEEE Trans. on Communication Technology, Vol. COM-17, p 138-161, April 1969.